PART II:
Molecular Structure, Vibrational Spectra and Photochemistry of 2-Methyl-2*H*-tetrazol-5-amine in Solid Argon

3.2.1. Introduction

When the substituent at the tetrazole ring carbon (at the 5-position) is an amino or imino group, photolysis can result in production of small C, N and H containing molecules of important astrophysical and/or industrial interest (*e.g.*, CN_2H_2, CN_3H or CNH_3 isomers). Since in our studies we wanted to avoid the complexity introduced by the presence of a labile hydrogen atom connected to the tetrazole ring, 2-methyl-2*H*-tetrazol-5-amine (2MTA; see Figure 1) was selected as a simple prototype molecule having the adequate characteristics for studying the photochemistry of amino/imino containing tetrazoles and their photoproducts, as well as their structural (including tautomerism) and vibrational properties. The main experimental method selected was infrared spectroscopy, together with the technique of isolation of the compound in a low temperature inert matrix. The interpretation of the experimental results was assisted by high-level molecular orbital calculations.

Accordingly, the molecular structure, infrared spectrum and UV photochemistry of 2-methyl-2*H*-tetrazol-5-amine (2MTA) isolated in solid argon (10 K) were investigated. The experimental results were supported by extensive DFT(B3LYP)/6-311++G(d,p) calculations. The infrared spectrum of matrix-isolated 2MTA was fully assigned and correlated with structural properties. Taking into consideration the observed frequency of the NH_2 wagging mode, it is suggested that, in the matrices, the amine group becomes slightly more planar than in the gas phase, due to matrix-packing effects. *In situ* UV-irradiation ($\lambda > 235$ nm) of the matrix isolated 2MTA monomer is

shown to induce three main primary photochemical processes: *(1)* tautomerization to mesoionic 3-methyl-1*H*-tetrazol-3-ium-5-aminide; *(2)* nitrogen elimination, with production of 1-methyl-1*H*-diazirene-3-amine; and *(3)* ring cleavage leading to production of methyl azide and cyanamide. Following the primary photoproducts, secondary reactions were observed, leading to spectroscopic observation of methylenimine and isocyanidric acid.

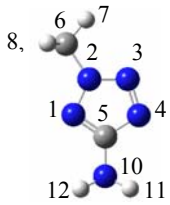

2-methyl-2*H*-tetrazol-5-amine

A **B**

3-methyl-1*H*-tetrazol-3-ium-5-aminide

A **B**

2-methyl-1,2-dihydro-5*H*-tetrazol-5-imine

A **B**

2-methyl-3*H*-tetrazol-2-ium-5-aminide

Figure 1. Calculated structures of 2-methyl-2*H*-tetrazol-5-amine (2MTA; with atom numbering) and of its imine (aminide) tautomers, 3-methyl-1*H*-tetrazol-3-ium-5 aminide, 2-methyl-1,2-dihydro-5*H*-tetrazol-5-imine and 2-methyl-3*H*-tetrazol-2-ium-5 aminide. In the case of the aminide tautomers, the placements of the charges on atoms correspond to one of the possible canonic forms for the mesoionic structures, which was also used to name the compound.

3.2.2. Results and Discussion

2-Methyl-2*H*-tetrazol-5-amine (2MTA) can exhibit tautomerism associated with the amine substituent. Indeed, hydrogen shift from the amino group to three different positions of the tetrazole ring leads to three possible pairs of tautomers bearing an imine (or aminide) NH substituent at position 5 (see Figure 1). Taking as reference the atom numbering of the tetrazole ring in 2MTA, the hydrogen involved in the tautomeric rearrangement can occupy the positions 1, 3 and 4 of the ring. In the first case tautomerism leads to the imine species, 2-methyl-1,2-dihydro-5*H*-tetrazol-5-imine, which can exist in two different conformations (A and B, in Figure 1), depending on the orientation of the imino hydrogen atom relatively to the tetrazole ring. The remaining two cases lead to mesoionic-type structures, 2-methyl-3*H*-tetrazol-2-ium-5-aminide and 3-methyl-1*H*-tetrazol-3-ium-5-aminide, respectively, that may also exist in two different stable conformations (see Figure 1). According to the calculations, all these tautomers of 2MTA have relative energies higher than 100 kJ mol^{-1} (Table 1), and are not expected to be significantly populated in the gaseous phase, within the temperature range employed in this study (< 90°C).

Table 1. Zero point vibrational energy (ZPVE) corrected DFT(B3LYP)/6-311++G(d,p) calculated energies (E_{ZPVE}/ Hartree) and relative energies (ΔE_{ZPVE}/ kJ mol^{-1}), including zero point energy corrections and dipole moments (|μ|/ Debye) for 2MTA and its 6 imino/aminide tautomers.

	E_{ZPVE}	ΔE_{ZPVE}	|μ|
2MTA	-352.945891	0.0	2.673
3-methyl-1*H*-tetrazol-3-ium-5-aminide (A)	-352.906166	104.3 (0.0)[a]	4.694
3-methyl-1*H*-tetrazol-3-ium-5-aminide (B)	-352.899621	121.5 (17.2)	5.185
2-methyl-1,2-dihydro-5*H*-tetrazol-5-imine (A)	-352.891460	142.9 (38.6)	6.218
2-methyl-1,2-dihydro-5*H*-tetrazol-5-imine (B)	-352.897524	123.6 (19.3)	4.299
2-methyl-3*H*-tetrazol-2-ium-5-aminide (A)	-352.855284	237.9 (133.6)	9.378
2-methyl-3*H*-tetrazol-2-ium-5-aminide (B)	-352.855697	236.8 (132.5)	9.134

[a] In parentheses: relative energies for the imino/aminide tautomers of 2MTA, taking as reference the lowest energy form.

It is interesting to note that the relative energies of the six imine (aminide) possible tautomers of 2MTA shown in Figure 1 seem to be essentially determined by the repulsions between the methyl or imine (aminide) hydrogen atoms and the hydrogen atom directly connected to the tetrazole ring. The two conformers of both iminide tautomers were found to be nearly planar. The close proximity of the methyl and tetrazole-ring hydrogen atoms in 2-methyl-3*H*-tetrazol-2-ium-5-aminide justifies the considerably higher energy of this tautomer. For this compound, the two conformers have very similar energies, due to the close resemblance of the two structures regarding intramolecular interactions (see Figure 1). On the other hand, the two conformers of 3-methyl-1*H*-tetrazol-3-ium-5-aminide differ in energy by 17.2 kJ mol^{-1}, because in conformer A the repulsion between the iminide and tetrazole-ring hydrogen atoms is absent. The imine tautomer exhibits both NH and NCH_3 nitrogen atoms pyramidalized [N–N(–CH_3)–N and N–N(–H)–C dihedral angles (defined as X-Y(-A)-Z, where A stays out-of-the-plane X-Y-Z) were estimated by the calculations as 133.4 and –124.3 degrees, for conformer A, and 136.3 and –128.6 degrees, for conformer B]. For this tautomer, the relative energies of the two conformers were also found to be influenced by the presence (in the less stable conformer A) or absence (in the more stable conformer B) of the repulsion between the imine and tetrazole-ring hydrogen atoms. 2MTA itself was found to have a planar tetrazole ring, with both the methyl carbon and amine nitrogen atoms lying in the ring-plane and the amine group pyramidalized (the calculated H–N(–C)–H dihedral angle was predicted to be 135.9 degrees). One of the methyl hydrogens is also in the ring plane, with the C–H bond eclipsing the $N_{(2)}$–$N_{(3)}$ bond, whereas the two remaining methyl hydrogen atoms occupy nearly symmetric positions above and below the plane of tetrazole ring. The complete equilibrium geometry of 2MTA is given in Table S1 (Appendix C).

- Infrared spectrum of the matrix isolated compound (as-deposited matrix)

The IR spectrum of 2MTA isolated in solid argon is presented in Figure 2, together with the B3LYP/6-311++G(d,p) calculated spectrum. Despite the fact that most of the bands in the experimental spectrum exhibit splitting due to matrix site effects, the agreement between the experimental and calculated spectra is very good, enabling us to fully assign the bands on the basis of the theoretical data. The assignments are provided in Table 2 [results of vibrational calculations for 2MTA and its 6 imine (amidine) tautomers, including the definition of the used internal coordinates, are provided in Tables S2-S10 (Appendix C)].

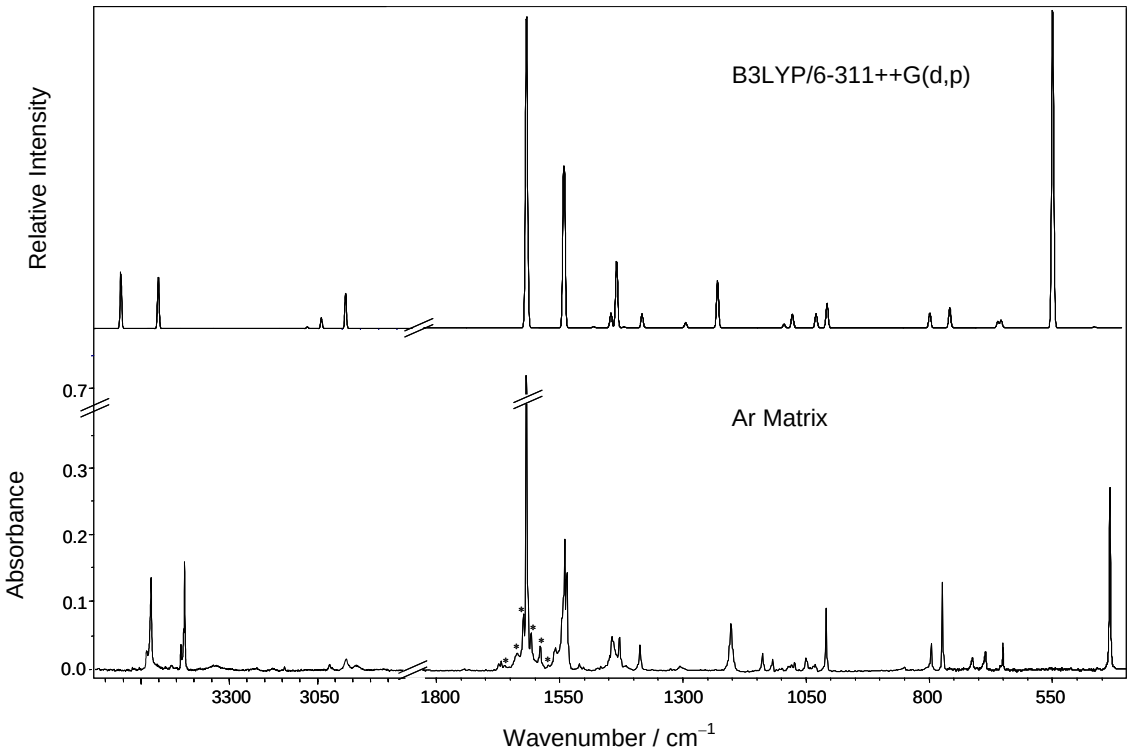

Figure 2. Infrared spectrum of 2MTA in an argon matrix (as-deposited matrix) and DFT(B3LYP)/ 6-311+G(d,p) calculated infrared spectrum. In the experimental spectrum, the asterisks indicate bands due to traces of isolated monomeric water. The calculated spectrum was simulated using Gaussian functions centered at the calculated frequency (scaled by 0.978) and with bandwidth at half-height equal to 5 cm^{-1}.

The following additional remarks shall be made:

a) No evidence for the presence in the matrix of any of the imine (aminide) tautomers of MTA was found.

b) The experimental spectrum contains minor bands due to traces of monomeric water, present in the system, which could not be avoided. However, it is clear from the positions of these bands[1] (see also Table 2) that water molecules were well isolated and do not interfere with the molecules of the compound under investigation.

c) Among all calculated (scaled) frequencies for the minimum energy conformation, the one showing the largest relative deviation relatively to the experimental value corresponds to the out-of-plane γNH_2 mode, which is *ca.* 25% overestimated by the calculations. Besides, the intensity of this band is also considerably overestimated. We investigated the dependence of the predicted spectra with the deviation of the amine group from planarity [the H–N(–C)–H dihedral angle was varied from 180.0 degrees (NH_2 group planar) to 100.0 degrees]. Note that in this particular case the calculated spectra for conformations other than the equilibrium one can still be considered meaningful since the γNH_2 vibration associated with change in the H–N(–C)–H dihedral angle couples significantly only with the δNH_2 coordinate [see Table S3 (Appendix C)]. For all non-equilibrium conformations, the forces coupling the out-of-plane γNH_2 with all other coordinates are negligible. Very interestingly, within the interval of variation considered, the spectrum practically did not change except in what concerns the frequency and IR intensity of the γNH_2 mode. Indeed, this vibration is strongly affected by the geometry of the amine group, both its frequency and intensity reducing in going from less planar to more planar geometries (Figure 3).

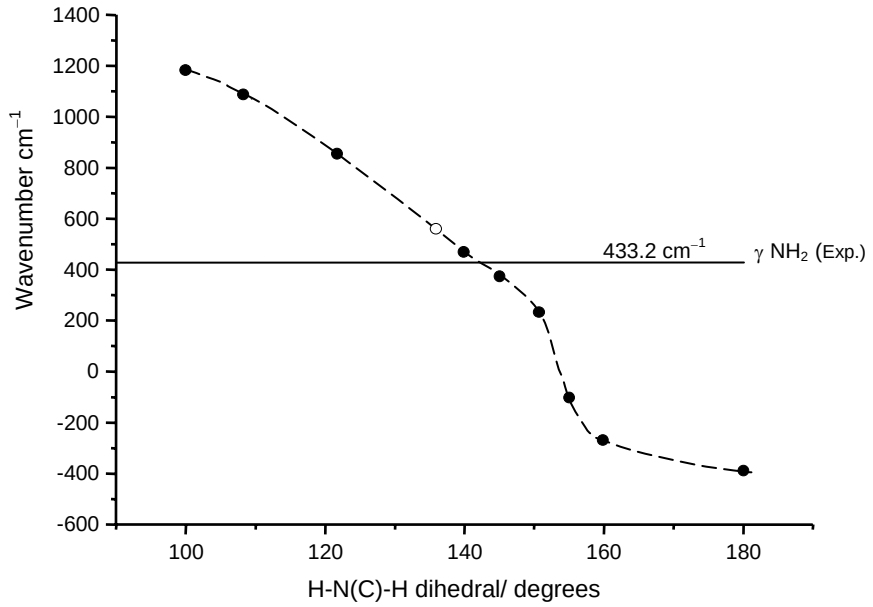

Figure 3. Dependence of the DFT(B3LYP)/6-311++G(d,p) calculated (scaled by 0.978) γNH_2 wavenumber on the H–N(C)–H dihedral angle (which is a measure of the degree of planarity of the amine group). The open circle corresponds to the minimum energy structure. Imaginary wavenumbers are represented by negative values.

The calculated frequency matches the observed one for a H–N(C)–H dihedral angle of 141.4 degrees (5.5 degrees more than the value corresponding to the calculated minimum energy conformation; note that for this geometry the energy was found to be only 0.395 kJ mol^{-1} higher than that of the minimum energy conformation). For this dihedral angle, the ratio of the calculated IR intensities of the two most intense bands in the spectrum [$I(\delta NH_2)/I(\gamma NH_2)$] is ≈ 2, close to the observed value of *ca.* 2.4, whereas the same ratio is calculated as nearly equal to unity for the minimum energy conformation. Hence, the data point to the occurrence of a change of geometry towards a more planar NH_2 group upon isolation of the molecule of 2MTA in the argon matrix. Stabilization of more planar structures in matrices (when compared with gas phase) is a relatively frequent phenomenon; it was observed previously, for example, for cyanoacetic acid and methyl[2,3] and benzyl[4] cyanoacetate.

Table 2. Experimental and calculated wavenumbers and intensities, and potential energy distribution (PED) for 2-methyl-2*H*-tetrazol-5-amine.[a]

Approximate description	Observed (Ar matrix)		Calculated [B3LYP/6-311++G(d,p)]		
	Wavenumber (cm^{-1})	Intensity (qualitative)[b]	Wavenumber (cm^{-1})	Intensity (km mol^{-1})	PED[c]
νNH_2 as + γNH_2	3960.4	w			
νNH_2 s + γNH_2	3863.8	w			
H_2O (monomer)	3776.7	w			
	3756.3	w			
	3738.6	vw			
	3724.7	vw			
	3711.6	w			
	3669.6	vw			
	3653.4	vw			
H_20 (dimer)	3574.0	vw			
νNH_2 as	3533.0	w	3606.2	44.4	S_{28}(100.0)
	3523.7	m; sh			
	3520.9	m			
νNH_2 s	3436.3	w	3503.8	40.1	S_{27}(99.9)
	3428.7	m; sh			
	3425.9	m			
	3345.2[d]	vw; b			
	3334.8[d]	vw; b			
2x δNH_2	3221.8	vw			
$\delta NH_2 + \nu C{=}N$	3143.7	vw			
νCH_3 as '	3015.2	vw	3095.6	1.1	S_9(97.2)
νCH_3 as "	2968.8	vw	3056.8	8.5	S_{10}(100.2)
νCH_3 s	2940.5	vw	2990.4	27.4	S_8(97.0)
2x ωNH_2	2212.2	vw			
$\nu N{-}N$ s + δring	2069.1	vw			
2x $\nu N{-}N$ s	2011.0	vw			
	2007.8	vw			
$\delta NH_2 + \tau CH_3$	1745.1	w			
$\nu C{=}N + \tau CH_3$	1673.2	vw			
	1669.4	vw			
H_2O (monomer)	1661.0	vw			
	1637.5	w			
	1624.6	m			
δNH_2	1618.0	S; sh	1617.7	262.0	S_{16}(49.3) + S_1(19.6) + S_{30}(18.0)
	1616.6	S			
H_2O (monomer)	1607.9	m			
	1605.9	w; sh			
	1592.9	vw			
	1589.8	w			
	1573.0	vw			
2x $\nu C{-}N(H_2)$	1560.8	w			
	1559.6	w; sh			
H_2O (monomer)	1557.6	w; sh			
$\nu C{=}N$	1545.6	m	1541.2	136.1	S_6(31.0) + S_{16}(26.0) + S_1(21.8) + S_{19}(9.6)
	1541.9	m			
	1539.9	S			
	1535.6	m			
δCH_3 as '	1509.8	vw	1480.3	0.7	S_{12}(68.3) + S_{14}(15.6)
	1502.3	vw			

Table 2 (Continued)[a]

νCH_3 as "	1449.5	w	1445.2	12.1	$S_{13}(90.5) + S_{15}(9.6)$
νN–C	1443.4	m	1433.3	55.6	$S_5(24.1) + S_{17}(17.2) + S_{12}(10.8) + S_{18}(9.8) + S_4(9.6)$
	1440.7	w; sh			
	1435.6	w; sh			
δCH_3 s	1428.6	w	1417.8	0.6	$S_{11}(89.0)$
$\nu N–C(H_3)$	1391.7	vw	1381.4	11.6	$S_2(38.9) + S_{20}(17.5) + S_7(16.1) + S_3(13.1)$
	1388.0	vw; sh			
	1386.0	w			
τring 1 + δring1	1325.0	vw			
νN–N as	1306.2	vw	1292.1	4.3	$S_3(29.1) + S_{14}(22.8) + S_7(17.1) + S_{12}(10.2)$
	1302.6	vw			
	1298.8	vw			
νN=N	1203.1	m	1226.9	39.9	$S_4(67.4) + S_{20}(19.4)$
	1198.7	w; sh			
τring 1 + γNH_2	1137.8	w			
γCH_3 "	1120.8	w; sh	1119.8	<0.1	$S_{15}(88.4) + S_{13}(9.6)$
	1118.0	w			
ωNH_2	1100.0	vw	1090.7	2.9	$S_{17}(31.9) + S_6(35.8) + S_{19}(9.9)$
δring 1 + γNH_2	1086.1	vw			
	1083.0	vw			
δring 2	1079.8	vw	1073.8	11.4	$S_{20}(20.4) + S_{17}(21.5) + S_7(12.6) + S_{19}(12.6) + S_5(14.1)$
	1073.8	vw			
γCH_3 "	1049.5	w	1025.2	11.8	$S_{14}(50.3) + S_3(21.1) + S_7(11.4)$
τring 1 + γring 1	1035.2	vw			
	1030.7	vw			
νN–N s	1013.9	vw	1002.7	20.4	$S_7(23.9) + S_5(38.6) + S_{19}(10.5) + S_3(10.3)$
	1010.1	w			
	1008.4	m			
2x γNH_2	851.0	vw			
$\nu C–N(H_2)$	797.6	w; sh	792.6	12.2	$S_1(22.0) + S_{19}(24.5) + S_2(19.7) + S_{20}(14.2)$
	795.6	m			
τring 2	772.5	S	751.4	16.7	$S_{24}(53.2) + S_{22}(40.2)$
$\omega N–(CH_3)_+$ γNH_2	712.6	w			
	711.6	w; sh			
τring 1	690.0	vw; sh	653.2	5.2	$S_{23}(98.2)$
	685.6	w			
δring 1	655.6	vw	646.6	6.2	$S_{19}(20.1) + S_2(32.7) + S_1(12.8) + S_{20}(11.8)$
	653.4	vw			
	651.5	vw; sh			
	650.1	w			
γNH_2	433.2	S	540.8	267.5	$S_{30}(71.2) + S_{16}(18.4)$
$\omega C–(NH_2)$	n.i.		455.2	0.6	$S_{18}(51.9) + S_{26}(35.9)$
γring 1			340.5	8.4	$S_{22}(43.6) + S_{24}(30.3) + S_{25}(19.7)$
τNH_2			310.7	2.7	$S_{29}(51.8) + S_{18}(10.7) + S_{26}(27.1)$
$\omega N–(CH_3)$			279.2	28.1	$S_{26}(24.1) + S_{29}(42.9) + S_{18}(23.6)$
γring 2			173.7	8.6	$S_{25}(82.3) + S_{22}(9.7) + S_{24}(9.7)$
τCH_3			103.8	<0.1	$S_{21}(100.9)$

[a] Bands due to traces of isolated monomeric H_2O were also observed in the as-deposited matrix. The corresponding wavenumbers are also provided in this table. ν, stretching; δ, bending; γ, rocking; ω, wagging; τ, torsion; s, symmetric; as, asymmetric.

[b] S, strong; m, medium; w, weak; vw, very weak; b, broad; sh, shoulder.

[c] See Table S2 (Appendix C) for definition of coordinates. Only PED values greater than 9.5% are given.

[d] Possibly originated in aggregated species.

- UV-irradiation experiments ($\lambda > 235$ nm)

The investigation of the photochemistry of the matrix-isolated 2MTA involved *in situ* UV-irradiation ($\lambda > 235$ nm) experiments. Upon irradiation, the bands due to 2MTA decrease in intensity, indicating that the compound is being transformed in other species, while new bands appear in the spectra. The changes are particularly noticeable in the 2300-1500 cm^{-1} spectral region, which is shown in Figure 4.

The photochemically induced opening of the tetrazole ring has been found to be an easy process.[5-13] As mentioned in Chapter 1, tetrazole itself easily eliminates molecular nitrogen, leading to production of nitrilimine, which then undergoes secondary photoreactions, such as isomerization to carbodiimide, cyanamide or a hydrogen cyanide/nitrene complex.[7]

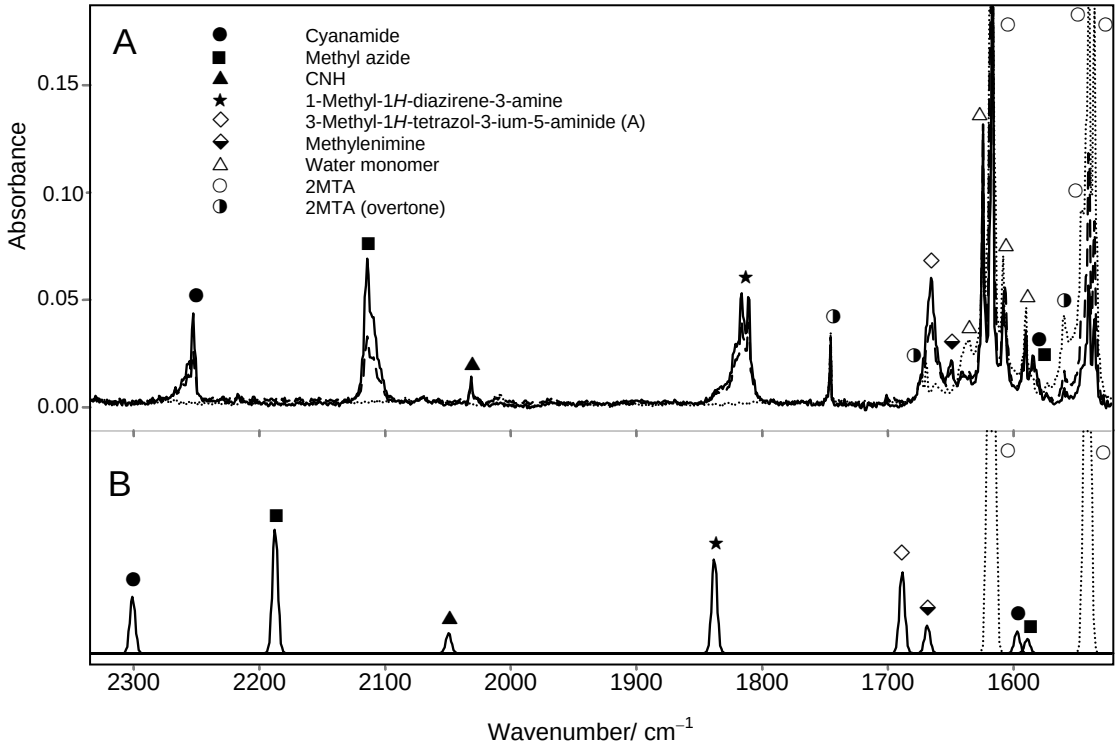

Figure 4. (A) 2300-1500 cm^{-1} region of the infrared spectra of the as-deposited argon matrix of 2MTA (dotted line) and of the UV-irradiated ($\lambda > 235$ nm) matrix after 80 min. (dashed line) and 160 min. (solid line) of irradiation. **(B)** DFT(B3LYP)/6-311++G(d,p) calculated (scaled by 0.978) infrared spectra of 2MTA and photoproducts in the same spectral region. In the calculated spectra, intensities for each molecule were scaled by different factors, to approximately simulate the corresponding observed intensities in the spectrum of the as-deposited matrix (2MTA) or of the 160 min. irradiated matrix (all products).

In the case of 2MTA, the weakest bonds of the tetrazole ring are $N_{(1)}$–$N_{(2)}$, $N_{(2)}$–$N_{(3)}$ and $N_{(4)}$–$C_{(5)}$, which correspond to the formal single bonds, and can then be expected to undergo easier photochemical cleavage. Simultaneous cleavage of the $N_{(1)}$–$N_{(2)}$ and $N_{(4)}$–$C_{(5)}$ bonds (in a [2+3] cycloelimination) would lead to production of methyl azide and cyanamide, while the analogous reaction involving breakage of the $N_{(2)}$–$N_{(3)}$ and $N_{(4)}$–$C_{(5)}$ bonds might produce either the cyclic diazirine (1-methyl-1*H*-diazirene-3-amine) or the open-ring nitrilimine (1-methyl-nitrilimine-3-amine), with simultaneous release of molecular nitrogen. Finally, the simultaneous cleavage of $N_{(1)}$–$N_{(2)}$ and $N_{(2)}$–$N_{(3)}$ bonds would produce methyl nitrene and triazet-4-amine. The IR spectra of all the above-mentioned putative photoproducts were calculated and compared with the new bands observed in the spectra of the photolysed matrix. Besides, available spectroscopic data for some of these species (methyl azide[14,15] and cyanamide)[16] were also taken into consideration. It was clear from these data that both cyanamide and methyl azide are among the photoproducts: the observed feature around 2260 cm^{-1} corresponds to the characteristic νNCN antisymmetric stretching band originated in cyanamide,[16] while methyl azide gives rise to the feature observed around 2100 cm^{-1} (νNNN antisymmetric stretching).[14,15] Other bands due to these two molecules expected to lie in the studied spectral range could also be identified in the spectra of the irradiated samples (a total of 9/13 bands for methyl azide and 5/6 bands for cyanamide; see Table 3), unequivocally demonstrating that simultaneous cleavage of the $N_{(1)}$–$N_{(2)}$ and $N_{(4)}$–$C_{(5)}$ bonds in the tetrazole ring of 2MTA took place upon irradiation. On the other hand, the feature appearing around 1815 cm^{-1} fits nicely the predicted frequency for the νNCN antisymmetric stretching vibration in 1-methyl-1*H*-diazirene-3-amine (see Figure 4 and Table 3). Indeed, it was possible to identify in the spectra of the irradiated matrix 11 out of the 14 bands of this species expected to lie in

the studied spectral range (see Table 3). Hence, nitrogen elimination through simultaneous cleavage of the $N_{(2)}$–$N_{(3)}$ and $N_{(4)}$–$C_{(5)}$ bonds did also occur, with production of the cyclic diazirine. No bands ascribable to the ring-open nitrilimine (CH_3–N=N^+=C^-–NH_2) were observed, nor those ascribable to the products of the simultaneous cleavage of $N_{(1)}$–$N_{(2)}$ and $N_{(2)}$–$N_{(3)}$ bonds (methyl nitrene and triazet-4-amine). This last result indicates that, if simultaneous cleavage of $N_{(1)}$–$N_{(2)}$ and $N_{(2)}$–$N_{(3)}$ bonds occurs, the primary photoproducts must undergo fast subsequent reactions. In this case, the most probable final products would be methylenimine, resulting from rearrangement of methyl nitrene, and cyanamide + N_2, resulting from opening of the four-membered ring of triazet-4-amine. I shall return to this point later on.

Besides the above-mentioned primary photoproducts, generation of other species upon irradiation of the matrix could also be established from the analysis of the spectra of the photolysed matrix. Two of these species are methylenimine and CNH. In the case of methylenimine, all but the νNH stretching vibration (predicted by the calculations as a very low intensity band –1.59 km.mol^{-1}) were identified (see Table 3). In the 2300-1500 cm^{-1} spectral region (see Figure 4) methylenimine gives rise to the band observed at 1649.5 cm^{-1}, ascribable to νCN. On the other hand, both the νNH and νCN bands of CNH were observed, the first at *ca.* 3580 cm^{-1} and the second around 2030 cm^{-1} (see Figure 4). The origin of these two products can be easily explained: it is well known that UV-induced decomposition of matrix isolated methyl azide gives rise to molecular nitrogen and methylenimine, through a concerted motion of N_2 elimination with hydrogen shift;[15,17,18] on the other hand, methylenimine can give CNH by 1,1-H_2 elimination, which was found to be a preferred route compared to 1,2-H_2 elimination giving HCN, 1,2-H shift yielding aminocarbene and N–H bond cleavage leading to the H_2CN radical.[17]

Table 3 – Assignments for the infrared bands due to photoproducts resulting from UV-irradiation ($\lambda > 235$) of 2MTA isolated in solid argon.[a]

Assignment	Approximate description	Wavenumber (cm^{-1})		
		Observed	Calculated[b]	Reference[c]
CNH	νN–H	3580.1 3576.8	3724.0(371)	3653
1-methyl-1*H*-diazirene-3-amine	νNH_2 as.	3536.0	3598.3(52)	
3-methyl-1*H*-tetrazol-3-ium-5-aminide (A)	$\nu N–H_{(12)}$		3588.8(118)	
cyanamide	νNH_2 as.	3528.1	3568.0(70)	3498
1-methyl-1*H*-diazirene-3-amine	νNH_2 s.	3445.0	3489.5(39)	
cyanamide	νNH_2 s.	3432.7	3477.1(44)	3401
methylenimine	νCH_2 as.	3084.8	3044.4(32)	3036
methyl azide	νCH_3 as. "	2995.9	3001.7(31)	2973
1-methyl-1*H*-diazirene-3-amine	νCH_3 as. "	2951.2	2996.2(22)	
methyl azide	νCH_3 s.	2922.9	2945.0(49)	2937
methylenimine	νCH_2 s.		2945.7(53)	2926
1-methyl-1*H*-diazirene-3-amine	νCH_3 s.	2896.9	2933.0(39)	
cyanamide	νNCN as.	2265.8 2260.4 2255.7 2251.8	2300.1(126)	2264
methyl azide	νNNN as.	2114.0 2110.4 2108.8 2104.2	2186.8(553)	2100
CNH	νCN	2031.2 2026.0	2049.2(74)	2024
1-methyl-1*H*-diazirene-3-amine	νNCN as.	1820.8 1815.9 1810.4	1837.7(280)	
3-methyl-1*H*-tetrazol-3-ium-5-aminide (A)	$\nu C–N(H_{(11)})$	1664.1	1680.9(721)	
methylenimine	νCN	1649.5	1668.6(25)	1641
cyanamide	δNH_2	1584.6	1596.9(48)	1586
1-methyl-1*H*-diazirene-3-amine	δNH_2		1588.8(42)	
1-methyl-1*H*-diazirene-3-amine	δCH_3 as. '	1466.0	1466.5(10)	
methyl azide	δCH_3 as. '	1458.0	1459.6(19)	1448
methylenimine	δCH_2		1459.5(7)	1453
1-methyl-1*H*-diazirene-3-amine	δCH_3 as. "	1435.6	1439.1(7)	
methyl azide	δCH_3 s.	1415.2	1419.8(7)	1405
3-methyl-1*H*-tetrazol-3-ium-5-aminide (A)	δCH_3 s.		1413.2(8)	
1-methyl-1*H*-diazirene-3-amine	δCH_3 s.	1406.9	1406.1(2)	
3-methyl-1*H*-tetrazol-3-ium-5-aminide (A)	$\delta NH_{(12)}$	1388.8	1370.6(27)	
1-methyl-1*H*-diazirene-3-amine	νNCN s.	1375.2 1371.3	1355.5(64)	
3-methyl-1*H*-tetrazol-3-ium-5-aminide (A)	$\nu N_{(1)}–N_{(2)}$	1359.2	1360.4(37)	
methylenimine	δNH	1357.6	1340.8(65)	1348
3-methyl-1*H*-tetrazol-3-ium-5-aminide (A)	$\delta N–H_{(11)}$	1305.1	1299.9(67)	
methyl azide	νNNN s.	1277.3 1272.9 1261.5	1310.3(132)	1270
3-methyl-1*H*-tetrazol-3-ium-5-aminide (A)	$\nu N_{(3)}–N_{(4)}$	1160.6	1154.4(75)	
methylenimine	γNH	1113.1	1136.3(47)	1123
methyl azide	γCH_3 '		1121.5(12)	1125
methylenimine	γCH_2	1071.9	1079.8(18)	1063

Table 3. (Continued)[a]

cyanamide	νNCN s.	1067.8	1072.3(10)	1061
methylenimine	ωCH_2	1040.2	1050.3(34)	1059
3-methyl-1*H*-tetrazol-3-ium-5-aminide (A)	γCH_3'		1044.4(100)	
3-methyl-1*H*-tetrazol-3-ium-5-aminide (A)	$\nu N_{(4)}–C_{(5)}$	981.8 977.1	940.1(53)	
methyl azide	νCN	892.1 887.0	896.0(20)	905
3-methyl-1*H*-tetrazol-3-ium-5-aminide (A)	δring 1	802.1 800.3	792.7(17)	
1-methyl-1*H*-diazirene-3-amine	γN(C)NN	~660	654.2(13)	660
methyl azide	δNNN		646.0(11)	
3-methyl-1*H*-tetrazol-3-ium-5-aminide (A)	$\nu N–C(H_3)$		643.2(20)	
3-methyl-1*H*-tetrazol-3-ium-5-aminide (A)	$\gamma N–H_{(12)}$	453.9	451.1(99)	

[a] ν, stretching; δ, bending; γ, rocking; ω, wagging; s., symmetric; as., antisymmetric. [b] DFT(B3LYP)/ 6-311++G(d,p) calculated values (scaled by 0.978) obtained in the present study. Numbers in parentheses are calculated intensities (km mol^{-1}). [c] Reference values correspond to previously reported experimental wavenumbers: cyanamide;[16] methyl azide;[14,15] methylenimine;[15,17-20] HNC.[21] Note that the photoproducts that are produced in the same matrix cage are interacting to each other; this leads to small, but measurable, differences in the observed wavenumbers, compared with those for the monomeric non-interacting compounds isolated in solid argon, provided here as reference values. For 3-methyl-1*H*-tetrazol-3-ium-5-aminide (A), the numbering of the atoms in the tetrazole ring follows that used for 2MTA; $H_{(11)}$ is the aminide hydrogen and $H_{(12)}$ the tetrazole-ring hydrogen [see Table S4 (Appendix C) for definition of coordinates for this molecule].

Another source of methylenimine (and, consequently, also of CNH) can be the photodecomposition of the primarily formed diazirine, which can undergo a ring-opening photoreaction leading to methylenimine and cyanamide, and the above-mentioned simultaneous cleavage of the $N_{(1)}–N_{(2)}$ and $N_{(2)}–N_{(3)}$ bonds of 2MTA. In these two cases, methyl nitrene shall act as intermediate. Note that the second putative primary photoproduct of simultaneous cleavage of the $N_{(1)}–N_{(2)}$ and $N_{(2)}–N_{(3)}$ bonds of 2MTA, triazet-4-amine, can be expected also to undergo subsequent photolysis leading to elimination of molecular nitrogen and formation of cyanamide. Hence, the occurrence of this process cannot be proposed beyond, since its expected final products can also be obtained through other reaction paths (which could be firmly established by identification of species that can only be produced in a unique way), and both putative precussor photoproducts (methyl nitrene and triazet-4-amine) could not be identified spectroscopically. Ring-opening processes involving cleavage of only one single bond

were also investigated. Among them, cleavage of the $N_{(2)}$–$N_{(3)}$ bond would lead to formation of 1-diazo-1-[methyldiazenyl]methanamine (CH_3–N=N–C(NH_2)=N^+=N^-), which was predicted to give rise to an intense band (νC=N=N antisymmetric stretching) at 2113 cm^{-1} (intensity: 535.6 km mol^{-1}). This vibration could also contribute to the band experimentally observed at 2031 cm^{-1}, ascribed to CNH (Table 3). Unfortunately all other vibrations of the methanamine were predicted by the calculations as giving rise to weak infrared bands. Hence, the possibility of occurrence of this process cannot be ruled out nor confirmed. An additional photoproduct could also be identified in the spectra of the irradiated matrix: conformer A of the 2MTA aminide tautomer, 3-methyl-1*H*-tetrazol-3-ium-5-aminide (see Figure 1), which can be obtained from 2MTA through a 1,3-H shift. In the 2300-1500 cm^{-1} spectral region, this species gives rise to the band at 1664.1 cm^{-1} (see Figure 4), but on the whole 11 out of the 28 bands of this species expected to lie in the studied spectral range were identified (see Table 3). Note that, as already mentioned in the text, this is the lowest energy imine/aminide tautomer of 2MTA. Besides, once formed it shall be comparatively less reactive to photolysis since N_2 elimination would also require an additional hydrogen atom migration. Furthermore, among the six possible imine/aminide tautomers, it is one of the two forms that can be directly produced from 2MTA as a result of an energetically accessible hydrogen-shift. The other is conformer B of 2-methyl-1,2-dihydro-5*H*-tetrazol-5-imine, which was not identified as contributing to the spectra of the irradiated matrix (this form is less stable than the observed species by *ca.* 20 kJ mol^{-1} and has a non-planar structure, then requiring a more important rearrangement of the matrix – see Figure 1 and Table 1). 1,4-H shift appears as an improbable process for the matrix isolated molecule and, thus, both conformers of 3-methyl-1*H*-tetrazol-3-ium-5-aminide are not expectable products (these are also the less stable among the 6 imine/aminide tautomers

of 2MTA; see Table 1). On the other hand, both conformer B of 3-methyl-1*H*-tetrazol-3-ium-5-aminide and conformer A of 2-methyl-1,2-dihydro-5*H*-tetrazol-5-imine have the wrong geometry for 1,3-H shift, requiring either an additional 180 degrees rotation about the C–N(H) bond or lateral migration of the imine (aminide) hydrogen atom and, furthermore, its production is not expected to be a favored process in a matrix. In summary, as depicted in Figure 5, photolysis of matrix-isolated 2MTA leads to *(1)* nitrogen elimination, with production of 1-methyl-1*H*-diazirene-3-amine; *(2)* ring cleavage leading to production of methyl azide and cyanamide; and *(3)* tautomerization to mesoionic 3-methyl-1*H*-tetrazol-3-ium-5-aminide in the A conformation. Following the primary photoproducts, secondary reactions were observed, leading to spectroscopic observation of methylenimine and isocyanic acid.

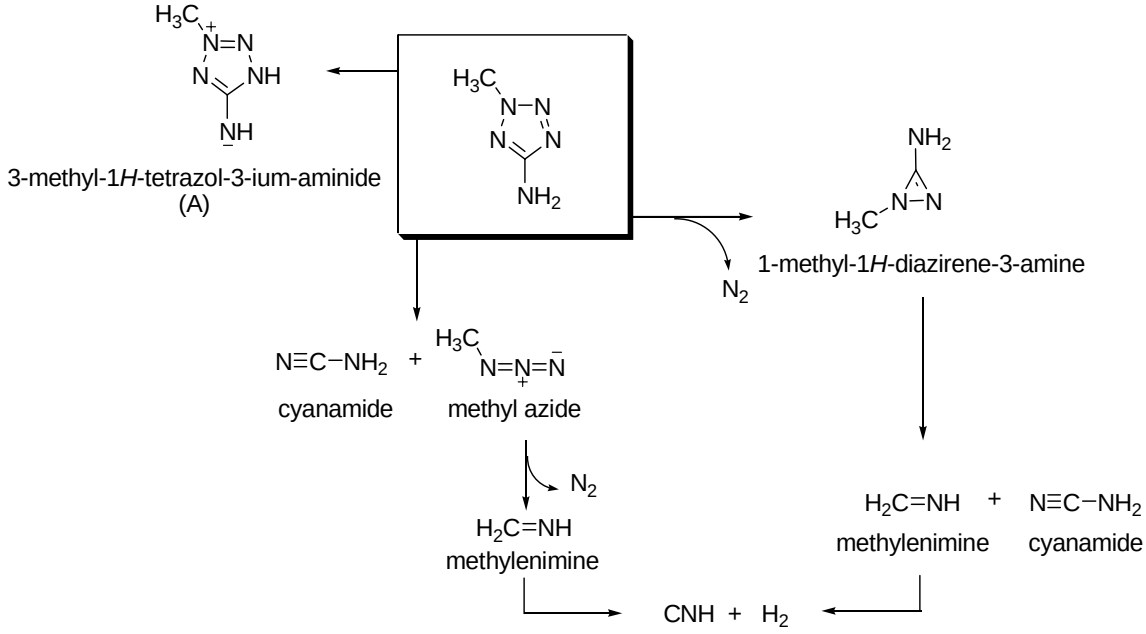

Figure 5. Photochemical reactions observed for 2-methyl-2*H*-tetrazol-5-amine isolated in cryogenic inert matrices upon irradiation with UV ($\lambda > 235$ nm) light.

Photochemical ring-opening leading to methyl nitrene and triazet-4-amine as primary photoproducts cannot also be discarded, but no firm evidence of this process could be established. Two additional points deserve here further comments. The first one results from the fact that, in a matrix, reactions are cage confined. Hence, these

processes lead necessarily to production of species that, once produced in the same matrix cage, shall interact with each other to some extent. In the present case, the precise nature of these interactions is not easily accessible, since up to 4 molecular species might co-exist in the same cage (*e.g.*, cyanamide + CNH + H_2 + N_2). However, their importance is clearly reflected in the fact that, in many cases, the observed frequencies for the photoproducts do not exactly match the reference frequencies for the isolated monomeric species in the same experimental conditions (see Table 3). The second point is related to the kinetics of the different processes observed. It can easily be concluded from Figure 6, which shows the change in the integral intensities (normalized by the corresponding calculated intensities) of characteristic bands of the various observed photoproducts with time of irradiation, that different products are formed at different rates and in different amounts. Among the three primary photoprocesses, nitrogen elimination with formation of 1-methyl-1*H*-diazirene-3-amine is the fastest reaction.

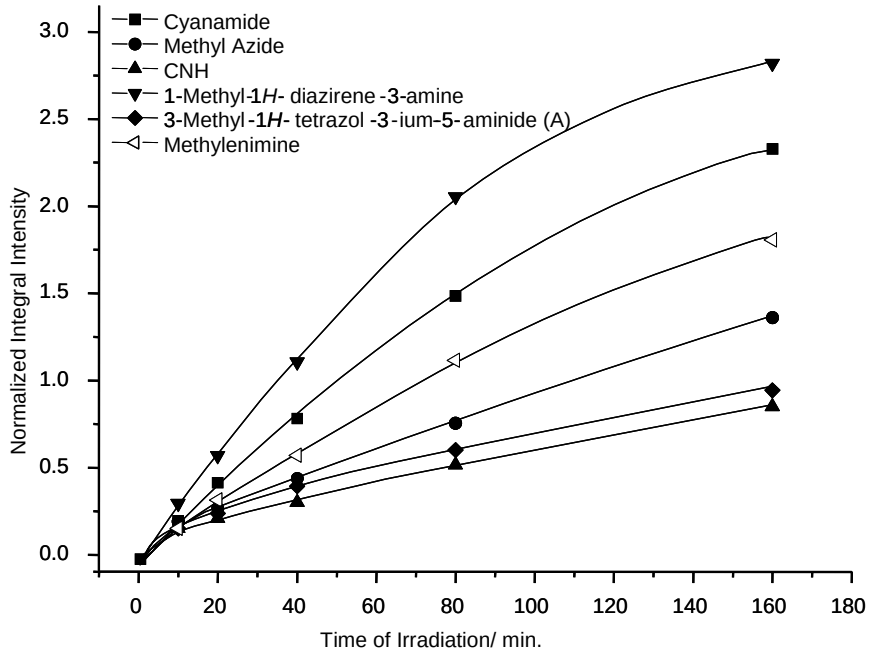

Figure 6. Variation with time of irradiation (min.) of the absorbances of the characteristic bands of 2MTA photoproducts, normalized by the corresponding calculated [DFT(B3LYP)/6-311++G(d,p) intensities].

The subsequent photodecomposition of 1-methyl-1*H*-diazirene-3-amine (to cyanamide and methylenimine) is also a comparatively fast process, since after 180 min. of irradiation the change in the amount of 1-methyl-1*H*-diazirene-3-amine is already small (see also Figure 4). The ring cleavage leading to production of methyl azide and cyanamide is considerably slower than the previously considered reaction and, after 180 min. of irradiation, the amount of methyl azide continues to grow almost linearly with time (Figures 4 and 6). Finally, the slowest observed primary photoprocess corresponds to the tautomerization of 2MTA to mesoionic 3-methyl-1*H*-tetrazol-3-ium-5-aminide. The fact that this last process is the slowest one among all observed processes may also indicate that 3-methyl-1*H*-tetrazol-3-ium-5-aminide is also being photoisomerized back to 2MTA.

▪ Conclusions

2-Methyl-2*H*-tetrazol-5-amine (2MTA) was found to have a planar tetrazole ring, with both the methyl carbon and the amine nitrogen atoms lying in the ring-plane and the amine group pyramidalized (the calculated H–N(–C)–H dihedral angle was predicted to be 135.9 degrees). The infrared spectrum of matrix-isolated 2MTA was fully assigned and correlated with structural properties, indicating that, in the matrices, the amine group becomes slightly more planar than in the gas phase, due to matrix-packing effects. *In situ* UV-irradiation ($\lambda > 235$ nm) of the matrix-isolated 2MTA monomer is shown to induce three main primary photochemical processes occurring at different rates: *(1)* tautomerization to mesoionic 3-methyl-1*H*-tetrazol-3-ium-5-aminide; *(2*) nitrogen elimination, with production of 1-methyl-1*H*-diazirene-3-amine; and *(3)* ring cleavage leading to production of methyl azide and cyanamide. Following the primary photoproducts, secondary reactions were observed, leading to spectroscopic observation of methylenimine and isocyanic acid.

3.2.3. Experimental Section

Equipment and experimental conditions. All chemicals were used as purchased from Aldrich. Solvents for extraction and chromatography were of technical grade. When required, the solvents used in reactions were freshly distilled from appropriate drying agents before use. Analytical TLC was performed with Merck silica gel 60 F_{254} plates. Melting points were recorded on a Stuart Scientific SMP3 melting point apparatus and are uncorrected. Mass spectra were obtained on a VG 7070E mass spectrometer by chemical ionization (CI). ^{1}H NMR (400 MHz) spectra were obtained on a Bruker AM-400 spectrometer using TMS the internal reference (δ = 0.0 ppm).

Infrared spectroscopy. The IR spectra were obtained using a Mattson (Infinity 60AR Series) Fourier Transform infrared spectrometer, equipped with a deuterated triglycine sulphate (DTGS) detector and a Ge/KBr beamsplitter, with 0.5 cm^{-1} resolution. Necessary modifications of the sample compartment of the spectrometer were carried out in order to accommodate the cryostat head and allow purging of the instrument by a stream of dry nitrogen to remove water vapors and CO_2. A solid sample of 2MTA was placed in a specially designed doubly thermostattable Knudsen cell.[22] Both the sample container and valve nozzle compartments of this cell were kept at 90°C during deposition. Matrices were prepared by co-deposition of 2MTA vapors coming out of the Knudsen cell together with large excess of the matrix gas (argon N60, obtained from Air Liquide) onto the CsI substrate of the cryostat, cooled to 10 K. Care was taken to keep the guest-to-host ratio in matrices low enough to avoid association. All experiments were performed using an APD Cryogenics close-cycle helium refrigeration system with a DE-202A expander. Irradiation of the samples was carried out with a 150 W xenon arc lamp (Osram XBO 150W/CR OFR). No changes in the

spectrum of the matrix-isolated 2MTA were observed during irradiation through a cut-off filter transmitting light above 337 nm.

Computational methodology. The quantum chemical calculations for 2MTA were performed with Gaussian 98 program package[23] at the DFT level of theory, using the 6-311++G(d,p) basis set and the three-parameter density functional abbreviated as B3LYP, which includes Becke's gradient exchange correction[24] and the Lee, Yang, Parr correlation functional.[25] The calculations on the possible photoproducts were carried out at the same level of theory. Geometrical parameters of the considered conformations were optimized using the Geometry Direct Inversion of the Invariant Subspace (GDIIS) method.[26] In order to assist the analysis of the experimental spectra, vibrational frequencies and IR intensities were also calculated with the same basis set. The computed harmonic frequencies were scaled down by a single factor (0.978) to correct them for the effects of basis set limitations, neglected part of electron correlation and anharmonicity effects. Normal coordinate analysis was undertaken in the internal coordinates space, as described by Schachtschneider,[27] using the program BALGA and the optimized geometries and harmonic force constants resulting from the DFT(B3LYP)/6-311++G(d,p) calculations.

Preparation of 2-methyl-2*H*-tetrazol-5-amine. A solution of sodium hydroxide (20%) was added dropwise to a suspension of tetrazol-5-amino monohydrate (10.3 g; 0.1 mol) in water (30 mL), with a drop of phenolphthalein. The mixture was stirred until complete dissolution of the suspended material. Dimethyl sulphate (20 mL; 0.11 mol) was then added in small portions, keeping an alkaline medium through addition of aqueous sodium hydroxide. The final mixture was refluxed for one hour, then cooled, filtered and the filtrate evaporated under reduced pressure to afford a solid residue. Water (50 mL) was added, and the mixture was then extracted with diethyl ether (3 × 50 mL). The organic extract was dried over anhydrous sodium sulphate, filtered and the filtrate evaporated to afford a light yellow oil that slowly crystallized. Recrystallization from diethyl ether gave the desired compound as colourless needles (25% yield), mp 103-104°C. ^{1}H NMR ($CDCl_3$): δ 4.15 (3H, s); MS (CI; NH_3): *m/z* 100 $[M+H]^+$, 117 $[M+NH_4]^+$.

3.3.4. References

1. Michaut, X.; Vasserot, A.-M.; Abouaf-Marguin, L. *Vib. Spectrosc.* **2004**, *34*, 83.
2. Reva, I.D.; Stepanian, S.G.; Adamowicz, L.; Fausto, R. *Chem. Phys. Lett.* **2003**, *374*, 631.
3. Reva, I.D.; Stepanian, S.G.; Adamowicz, L.; Fausto, R. *J. Phys. Chem. A* **2003**, *107*, 6351.
4. Lopes, S.; Gómez-Zavaglia, A.; Lapinski, L.; Chattopadhyay, N.; Fausto, R. *J. Phys. Chem. A.* **2004**, *108*, 8256.
5. Dunkin, I.R.; Shields, C.J.; Quast, H. *Tetrahedron* **1989**, *45*, 259.
6. Chae, Y.B.; Chang, K.S.; Kim, S.S. *The Daehan Hwak Hwoejee* **1967**, *11*, 85.
7. Maier, G.; Eckwert, J.; Bothur, A.; Reisenauer, H.P.; Schmidt, C. *Leibigs Ann.*, **1996**, 1041.
8. Awadallah, A.; Kowski, K.; Rademacher, P. *J. Heterocycl. Chem.* **1997**, *34*, 113.
9. Quast, H.; Bieber, L. *Angew. Chem.-Int. Edit. Engl.* **1975**, *14*, 428.
10. Quast, H.; Bieber, L. *Chem. Ber.-Recl.* **1981**, *114*, 3253.
11. Quast, H.; Fuss, A.; Nahr, U. *Chem. Ber.-Recl.* **1985**, *118*, 2164.
12. Quast, H.; Nahr, U. *Chem. Ber.-Recl.* **1985**, *118*, 526.
13. Quast, H. *Heterocycles* **1980**, *14*, 1677.
14. Zhizhong, W. *J. Mol. Struct.(Theochem.)* **1998**, *434*, 1.
15. Milligan, D.E. *J. Chem. Phys.* **1961**, *35*, 1491.

16. King, S.T.; Strope, J. H. *J. Chem. Phys.* **1971**, *54*, 1289.
17. Nguyen, M.T.; Sengupta, D.; Ha, T.-K. *J. Phys. Chem.* **1996**, *100*, 6499.
18. Nguyen, M.T. *Chem. Phys. Lett.* **1985**, *117*, 290.
19. Jacox, M.E.; Milligan, D. E. *J. Mol. Spectrosc.* **1975**, *56*, 333.
20. Oliveira, G.; Martins, J.M.L.; Silwa, I.K.S.; Liebman, J.F. *J. Comput. Chem.* **2001**, *22*, 1297.
21. Crovisier, J., BASEMOL - *"Constants for Molecules of Astrophysics Interest in the Gas Phase: Photodissociation, Microwave and Infrared Spectra"*, Laboratoire d'études spatiales et d'instrumentation en astrophysique, Observatoire de Paris-Meudon, France. (2002). http://www.usr.obspm.fr/~crovisie/basemole/
22. Reva, I.; Stepanian, S.; Adamowicz, L.; Fausto, R. *J. Phys. Chem. A* **2001**, *105*, 4773.
23. Frisch, M.; Trucks, G.; Schlegel, H.; Scuseria, G.; Robb, M.; Cheeseman, J.; Zakrzewski, V.; Montgomery, J.; Stratmann, R.; Burant, K.; Dapprich, S.; Millam, J.; Daniels, A.; Kudin, K.; Strain, M.; Farkas, O.; Tomasi, J.; Barone, V.; Cossi, M.; Cammi, R.; Mennucci, B.; Pomelli, C.; Adamo, C.; Clifford, S.; Ochterski, J.; Petersson, G.; Ayala, P.; Cui, Q.; Morokuma, K.; Malick, D.; Rabuck, A.; Raghavachari, K.; Foresman, J.; Cioslowski, J.; Ortiz, J.; Baboul, A.; Stefanov, B.; Liu, G.; Liashenko, A.; Piskorz, P.; Komaromi, I.; Gomperts, R.; Martin, R.; Fox, D.; Keith, T.; Al-Laham, M.; Peng, C.; Nanayakkara, A.; Challacombe, M.; Gill, P.; Johnson, B.; Chen, W.; Wong, M.; Andres, J.; Gonzalez, C.; Head-Gordon, M.; Replogle, S.; Pople, J. Gaussian 98, revision A.9, Gaussian Inc.: Pittsburgh, PA (1998).
24. Becke, A.D. *Phys. Rev. A* **1988**, *38*, 3098.
25. Lee, C.T.; Yang, W.T.; Parr, R.G. *Phys. Review B* **1988**, *37*, 785.
26. Csaszar, P.; Pulay, P. *J. Mol. Struct. (Theochem.)* **1984**, *114*, 31.
27. Schachtschneider, J.H.; Technical Report, Shell Development Co. Emeryville, CA, (1969).